Published by Avanti Publishers

Journal of Advances in Applied & Computational Mathematics

ISSN (online): 2409-5761

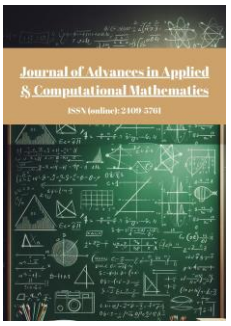

Accurate Estimation of COVID-19 Active Cases Using Bézier Curve-Based Mathematical Modeling

Emre Eroglu*

Department of Mathematics, Kirklareli University, Kırklareli 39100, Turkey

ARTICLE INFO

Article Type: Research Article

Academic Editor: Youssef Raffoul

Keywords:
COVID-19
Bézier curve
Pandemic forecasting
Active case estimation
Data-driven prediction
Mathematical modeling
Epidemiological modeling

Timeline:
Received: October 30, 2025
Accepted: December 12, 2025
Published: December 28, 2025

Citation: Eroglu E. Accurate estimation of COVID-19 active cases using Bézier curve-based mathematical modeling. J Adv Appl Computat Math. 2025; 12: 217-230.

DOI: https://doi.org/10.15377/2409-5761.2025.12.13

ABSTRACT

COVID-19 has reminded humanity of the devastating reality of a pandemic after many years. This global crisis fundamentally altered daily life and exposed significant vulnerabilities in public health systems worldwide. This work proposes a geometric curve-based prototype to support the fight against current and future pandemics. The study models a near-perfect estimation of the active case number with the help of the Bézier curve. The Bézier prototype consists of a C0 class, piecewise continuous, and segmented structure. The noiseless and cost-free model estimates the number of active cases in Germany, Canada, and Israel with minimum error. It compares the results obtained with those of cases in China. The absolute average error of the model is reduced to 0.087%. As a result, the consistent and cost-effective model can increase the likelihood of making rapid and accurate decisions against epidemics, produce well-organized projections for the future, and improve the effectiveness of measures to be taken.

*Corresponding Author
Email: eroglumre@gmail.com
Tel: +(90) 553 662 11 22

1. Introduction

To briefly mention, five years ago, COVID-19 [1-11], which emerged at the beginning of 2020, spread to all continents in a short time and has become a pandemic. The pandemic can be addressed from different perspectives, such as the effects it has caused worldwide, the burden on healthcare systems, and economic and social consequences. The impact of COVID-19 on healthcare systems has varied significantly depending on the healthcare infrastructure and preparedness levels of countries. However, even in developed countries, one may observe serious problems with basic healthcare needs, such as hospitals, intensive care units, and ventilators [12]. The disease, which has surpassed the significant struggle of healthcare workers against the virus at the cost of their lives, has led to the collapse of systems almost everywhere and the loss of many lives. The troubles of developing countries have been compounded not only by the speed at which the virus spreads but also by limited resources and insufficient testing capacity. The pandemic has been brought under control more slowly in these countries [13]. The pandemic has had a major impact on the global economy [12]. Global trade is severely weakened due to production and travel restrictions. Although countries offer financial stimulus packages to ease economic hardship, this cannot prevent unemployment from rising. COVID-19 also affects social-human interaction [14]. Schools are closed, and distance education is introduced. Increasing income inequality in the process leads to social injustice. One of the most important steps in controlling the process is the development of vaccines [15]. A relative relief is provided via vaccines developed by researchers who do not have enough time, which should be a separate issue of discussion. However, the failure to provide a homogeneous distribution around the world related to access to vaccines appears as another factor that deepens social imbalance. While developed countries have the chance to vaccinate earlier, access to vaccines is limited in relatively low-income countries. This situation brings the problem of global vaccine inequality to the agenda [16-19].

This manuscript introduces a new approach on COVID-19 modeling. It constructs a prototype of the patient numbers for Germany, Canada, and Israel based on active cases using the Bézier curve and cross-checks this model with data from China. The Bézier curve model is a parametric, segmented, and adaptive model.

Germany [12, 20], which has a strong health system, is one of the countries that has relatively well controlled the spread of the virus. However, capacity problems in intensive care units have caused concerns in the early stages of the pandemic. When compared to European countries, with the effect of the Pfizer/Biontech vaccine produced in the country, Germany's success in this sense can be said. Nevertheless, the first period of the pandemic is also difficult for Germany, especially due to the loss of labor and economic contraction.

Glancing at Canada [12, 21], a high standard of living reflected in the social healthcare system, which has some particular problems, is noticed in the country. The country, which also exhibits successful management in vaccination, quickly reaches its people with extensive vaccination campaigns. Canada has become one of the countries that has taken important measures in the fight against the pandemic by restricting border crossings.

Israel [12, 22], which has a reputation in the world related to genomics and biological studies, is also one of the leaders in vaccination. The strict implementation of social measures, together with masking, slows down the rate of spread of the pandemic in Israel. With the rapid vaccination, the decreasing spreading speed of the pandemic is observed relatively faster than in other countries.

China [12, 23-25], the country where the pandemic first emerged, struggles with keeping the spread of the virus under control with strict quarantine measures. The country declares a “zero COVID” strategy in the early stages. The country’s large population causes remarkable problems for the country. In terms of vaccination, the Chinese state has launched a large vaccination campaign using its own Sinopharm and Sinopharm vaccines.

The work includes an introduction, material and method, discussion, and conclusion sections.

2. Data and Theoretical Background

2.1. Basic Statistical Appearance

This study is based on data (active case) from the Worldometer (https://www.worldometers.info/ (April 26, 2020)). These data belong between February 15 and April 26, 2020. First, a brief definition is presented for the data. With

descriptive analysis (Table **1**), the data's change ranges, standard deviations, and variances are displayed. Table **2** expresses the binary relationship of the data. Fig. (**1**) is the hierarchical cluster view. In Table **3**, the standard of data distribution is observed.

Table 1: Descriptive rates.

	Min.	Max.	Mean	Std. Deviation	Variance
China	38505	1908936	577230.26	634801.302	402972693293.605
Germany	16	157770	54063.17	59333.965	3520519413.268
Canada	8	46895	10639.83	14455.184	208952353.099
Israel	1	15443	4621.08	5546.354	30762043.204

Table **1** shows the standard deviation and variance of the data in addition to their minimum and maximum values.

Table **2** denotes the binary correlation of the data. This score is strong when it is closer to one. Correlation constants are strong for countries. One may infer that the active case scores of Germany, Canada, Israel, and China are strongly correlated with each other.

Table 2: Correlation matrix.

	China	Germany	Canada	Israel
China	1	.991**	.987**	.998**
Germany		1	.957**	.994**
Canada			1	.980**
Israel				1

**. Correlation is significant at the 0.01 level (2-tailed).

Fig. (**1**) illustrates the hierarchy of data through linear paths.

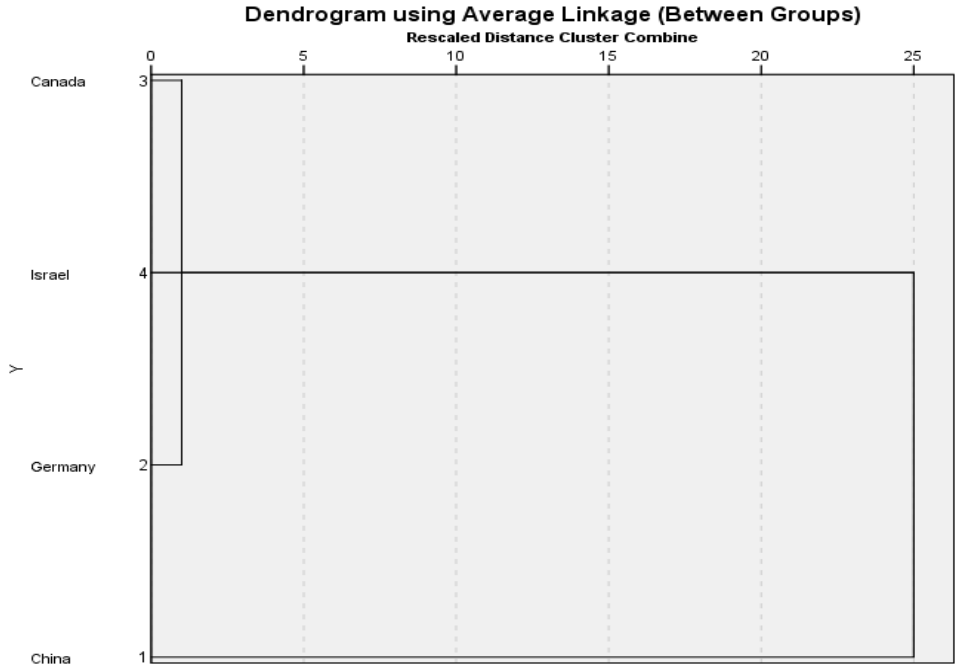

Figure 1: Hierarchical cluster of data.

According to Fig. (**1**), there are three main clusters in the data. One is for Germany, Israel, and Canada, and the other is for China. The third relationship is the Israel-China relationship.

Kaiser-Mayer Olkin (KMO)-Bartlett Test expresses the distribution of the data set. This test, used under factor analysis, explains the suitability of the data for analysis. The test score is evaluated between 0 and 1. As this score approaches 1, the normal distribution of the data can be mentioned more clearly. A score above 0.5 is generally expected for the observation of the normal distribution of the data. The significance in the table is desired to be less than 0.05.

Table 3: KMO and Bartlett's test.

Kaiser-Meyer-Olkin Measure of Sampling Adequacy.		.668
Bartlett's Test of Sphericity	Approx. Chi-Square	1194.187
	df	6
	Sig.	.000

According to Table **3**, active case data of the countries have a normal distribution.

2.2. Bézier Curve Modeling

This section discusses the curve model of the dataset. The prototype of the prediction of COVID-19 active cases is modeled using the Bézier curve. The model, proposed by the French engineer Pierre Bézier [26] in the early 1970s, has found its place in many applications, from surface design to curve fitting, from graphic modeling to image processing. Fig. (**2**) denotes a few types of curves.

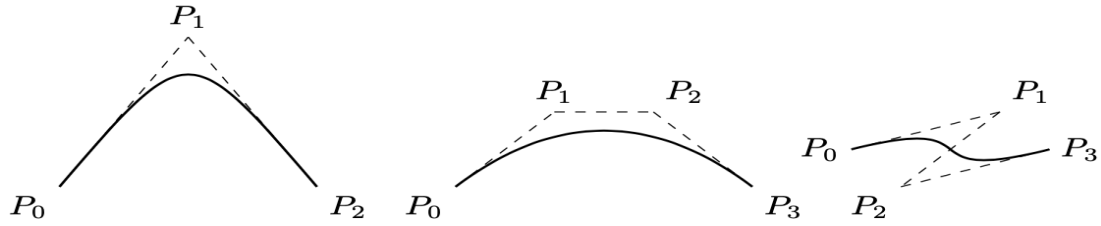

Figure 2: Bézier samples.

The segmented structure [27] with parametric curve behavior is mobile, flexible, and adaptable with control points. In each segment, the intermediate points of the curve, which include the starting and ending points, are free. Intermediate points are usually not selected on the curve. Traditionally, intermediate points are determined by methods such as median, least squares, etc. This paper`s intermediate points are calculated by the average of the data for every segment. The curve, which is parameterized between 0 and 1, has excellent flexibility with control points. Since each segment of the curve is connected, the structure is piecewise continuous. Moreover, the starting and ending points of successive segments make the structure a class C^0 geometric structure [28]. That is, the ending point of the previous segment is the same as the starting point of the following segment.

The differential geometrical curve can be presented by the binomial expansion $(x+y)^n = \sum_{k=0}^{n} \binom{n}{k} x^k y^{n-k}$ and the Bernstein polynomial $B(u) = \sum_{k=0}^{n} \binom{n}{k} (1-u)^{n-k} u^k$. Provided that P_k are checkpoints and parameter u from $0 \le u \le 1$, the n-degree general Bézier model is:

$$\mathfrak{B}(u) = \sum_{k=0}^{n} \binom{n}{k} (1-u)^{n-k} u^k P_k. \quad (1)$$

The difference between the number of control points of a curve and its degree is 1. A quadratic curve has three control points, and a cubic has four control points. An n-degree curve has n+1 points. The Bézier is invariant at the affine frame [29]. From eq. (1), one may see that $\mathfrak{B}(0) = \mathfrak{B}(1) = 0$. In this work, the prediction models for the number

of active cases are governed by the cubic Bézier curve. Provided that free parameter $u \in [0,1]$ and P_k, k=0,1,2,3, are the checkpoints, the cubic prototype and its matrix form are:

$$\mathfrak{B}(u) = \sum_{k=0}^{n} \frac{n!}{k!(n-k)!} u^k (1-u)^{n-k} P_k \tag{2}$$

$$\mathfrak{B}(u) = (u^3 \;\; u^2 \;\; u \;\; 1)_{1x4} \cdot \begin{pmatrix} -1 & 3 & -3 & 1 \\ 3 & -6 & 3 & 0 \\ -3 & 3 & 0 & 0 \\ 1 & 0 & 0 & 0 \end{pmatrix}_{4x4} \cdot \begin{pmatrix} P_0 \\ P_1 \\ P_2 \\ P_3 \end{pmatrix}_{4x1} \tag{3}$$

The third-degree curve [30, 31] is quite successful in modeling problems related to dynamic systems. In each segment of the cubic Bézier curve, the first and fourth points belong to the curve, while the second and third points are free. While the curve gets its flexibility and adaptability from its intermediate points, the starting and ending points also provide piecewise continuity to the structure. In this way, the structure offers both excellent estimation (modeling) opportunity by exhibiting fragmentary behavior and enables the general observation of the problem by acting as a whole. In this subsection, basic geometric invariants are given to exhibit the behavior of the curve. The theorem exhibits the first three degrees of derivatives of Bézier.

Theorem: The $\mathfrak{B}(u)$ Bézier curve derivatives are:

$$\begin{aligned} \mathfrak{B}'(u) &= n \sum_{k=0}^{n-1} B_{n-1,k}(u) \mathfrak{D}_1 P_k \\ \mathfrak{B}''(u) &= n(n-1) \sum_{k=0}^{n-2} B_{n-2,k}(u) \mathfrak{D}_2 P_k \\ \mathfrak{B}'''(u) &= n(n-1)(n-2) \sum_{k=0}^{n-3} B_{n-3,k}(u) \mathfrak{D}_3 P_k \end{aligned} \tag{4}$$

in where the Bernstein polynomial is $B_{n,k}$ and $\mathfrak{D}_0 = P_1 - P_0$, $\mathfrak{D}_1 = P_2 - P_1$, $\mathfrak{D}_2 = P_3 - P_2, \ldots, \mathfrak{D}_k = P_{k+1} - P_k$ [32]. One can realize that the r order derivatives from eq. (5) and (6) with u=0 and u=1 are:

$$\mathfrak{B}^r(u)_{|u=0} = \frac{n!}{(n-r)!} \sum_{k=0}^{r} (-1)^{r-k} \binom{r}{k} P_k \tag{5}$$

$$\mathfrak{B}^r(u)_{|u=1} = \frac{n!}{(n-r)!} \sum_{k=0}^{r} (-1)^{k} \binom{r}{k} P_{n-k}. \tag{6}$$

According to eq. (5-6), the initial and terminal checkpoints are tangent to the curve. In this last subsection, the particular geometric invariants from the Frenet-Serret frame are handled. The mentioned provides a generic insight into the behaviors of the curve. The Serret-Frenet frame contains the unit vectors *tangent*, *normal*, *and binormal unit vectors* (**T**, **N**, **B**), the *curvature* (**K**), and the *torsion* (**Ƭ**) functions.

Suppose that α is a unit speed, α from $[0,1]$ to $\mathbb{R}^n$, and u is a free parameter between $[0,1]$. One knows that when a curve is known to have unit speed, then $\|\alpha'(u)\| = 1$ for the norm $\|\ldots\|$. For the Frenet frame, the tangent unit vector $\mathbf{T}(u) = \alpha'(u)$. With the rushing, one obtains $\mathbf{T}'(u) = \alpha''(u)$, where curvature κ is denoted by $\|\mathbf{T}'(u)\|$ norm for each $u \in [0,1]$. The curvature function $\kappa(u)$ is a real function for the α curve. It denotes the deviation of the tangent. For the $\kappa(u) > 0$, the normal unit vector field **N** is formulated by $\mathbf{N}(u) = \frac{\mathbf{T}'(u)}{\|\mathbf{T}'(u)\|} = \frac{\mathbf{T}'(u)}{\kappa(u)}$. The binormal vector of the α curve is denoted by $\mathbf{B}(u) = \mathbf{T}(u) \times \mathbf{N}(u)$. The curvature is showed by $\kappa(u) = \frac{\|\mathfrak{B}'(u) \times \mathfrak{B}''(u)\|}{\|\mathfrak{B}'(u)\|^3}$ and the τ scalar torsion function of the α curve is denoted by $\tau(u) = \mathbf{B}'(u).\mathbf{N}(u)$. The following lemma expresses the geometric positions of the three vectors.

Lemma: Suppose that α is a unit speed curve and curvature $\kappa > 0$ on $\mathbb{R}$. The (**T**, **N**, **B**) vectors, which constitute the Frenet frame for the curve, on the α curve are perpendicular to each other for all space points.

2.3. Bézier Curves and Rationale for Epidemiological Modeling

Why Bézier curve estimation model? With a wide range of applications and a fresh approach to the number of active cases, Bézier is particularly practical and innovative compared to other models. Table **4** provides a brief evaluation of other estimation methods and the proposed curved approach. The table allows the reader to compare the models.

Table 4: Comparison to the other estimation approaches.

Model	Data Requirement	Assumption	Computational Cost	Sensitivity to Noise	Explainability	Suitability for Rapid Pandemic Monitoring
ARIMA	Medium	Linear time-series structure	Medium	High	Medium	Moderate
Nonlinear Regression	Low–Medium	Fixed functional form	Low	Medium	High	Low–Moderate
SIR/SIRD	Low–Medium	Epidemic parameters (β, γ, δ) assumed constant	Medium	High	Medium	Moderate
Deep Learning	Very high	None, but opaque	Very high	Very high	Very low	Variable
Proposal	Low	None (purely geometric)	Very low	Low (smooth C^0 class reduce noise)	High (deterministic geometry)	Excellent

The reader can observe the estimation model, data requirement of the model, assumption technique, computational cost, sensitivity to noise, explainability of the model, and suitability for rapid pandemic monitoring of the model in Table **4**.

Bézier curves constitute a fundamental class of parametric curves widely used in geometric modeling, computer-aided design, and data approximation due to their mathematical simplicity, numerical stability, and strong geometric interpretability. In this study, Bézier curves are employed as a functional data analysis tool to model the temporal evolution of COVID-19 active case numbers with high precision.

The control points play a central role in shaping the curve. Rather than interpolating all data points, the Bézier curve approximates the data by adjusting the position of its control points, which allows smooth global control of the curve's behavior. A key geometric property is the convex hull property: the entire curve lies within the convex hull of its control points. This ensures numerical stability and prevents unrealistic oscillations, which is particularly important when modeling epidemiological data that must preserve monotonicity and boundedness over time.

Continuity properties are essential when modeling time-dependent phenomena. Bézier curves support different continuity classes depending on how curve segments are connected. In this study, a piecewise C^0-continuous segmented structure is employed, meaning that curve segments join without breaks while allowing local flexibility. Higher-order continuity (C^1 or C^2), which enforces smooth first or second derivatives, can also be imposed if required, but C^0 continuity is sufficient and advantageous for capturing abrupt changes in epidemic dynamics caused by interventions, reporting delays, or policy shifts.

The parametric nature of Bézier curves enables a clear separation between time (parameter t) and state variables (active case numbers). This parametric representation allows efficient approximation of nonlinear temporal trends without assuming an underlying stochastic process or epidemiological compartmental structure. Unlike regression-based or differential equation–based models, Bézier curves do not require prior assumptions about transmission rates, recovery parameters, or population mixing, making them particularly suitable for data-driven modeling under uncertainty.

Bernstein polynomials form the numerical backbone of Bézier curves and contribute significantly to their robustness. These polynomials are non-negative over the interval [0,1] and sum to unity, which ensures numerical stability and smooth approximation behavior. Their well-conditioned nature reduces sensitivity to noise and rounding errors, a crucial advantage when dealing with real-world pandemic data that may contain inconsistencies or reporting artifacts.

Overall, the mathematical formulation and geometric properties of Bézier curves provide a stable, flexible, and interpretable framework for modeling epidemic trajectories. Their ability to approximate complex temporal patterns using a small number of parameters, combined with their continuity control and numerical stability, makes them a powerful alternative to traditional epidemiological and statistical models in pandemic data analysis.

2.4. Implementation Overview

To ensure transparency and reproducibility, a simplified implementation pipeline is outlined. The procedure involves: (1) segmentation of the time series into fixed 12-hour windows; (2) construction of cubic Bézier segments using reported active case values as control points; (3) computation of parametric curve trajectories for each segment; (4) evaluation of model performance using mean absolute error per segment; and (5) optional adaptive re-segmentation for segments exhibiting maximal deviation. This overview is intended to facilitate.

3. Results and Discussion

T, **N**, **B** vectors representing the tangent, normal, and binormal vectors along a space curve provides a powerful geometric tool for describing the local behavior of trajectories and surfaces. Its associated parameters—curvature (κ) and torsion (τ)—quantify how a curve bends and twists in three-dimensional space. Beyond pure geometry, these quantities have become essential descriptors in contemporary modeling and data analysis across multiple disciplines.

In engineering and robotics, the Frenet frame is widely used in trajectory planning and motion control. When designing the path of an autonomous vehicle, drone, or robotic arm, the curvature determines how sharply the system must turn, while the torsion governs how the path deviates from a plane. By optimizing these quantities, engineers can minimize energy consumption, ensure mechanical stability, and avoid abrupt changes in motion that could damage hardware or reduce accuracy.

In computer graphics and animation, curvature and torsion form the mathematical backbone of realistic motion and shape generation. Bézier and spline curves, often utilized for surface modeling, rely on local curvature control to achieve smooth transitions between segments. The Frenet frame allows the precise definition of surface normals and shading directions, which is essential for realistic rendering and dynamic deformation of 3D objects.

In biomechanics and medical imaging, the Frenet–Serret apparatus is used to model the geometry of biological structures such as blood vessels, DNA strands, or spinal curvature. The curvature indicates how sharply a structure bends, while torsion measures its spatial twisting, which are critical parameters in understanding flow dynamics, structural stress, and morphological disorders. This approach aids in diagnostic modeling and in the design of bio-inspired materials or prosthetics.

In atmospheric and environmental modeling, the Frenet frame can describe the geometric behavior of streamlines in wind flow, ocean currents, or pollutant dispersion paths. The curvature corresponds to the rate of directional change of a flow trajectory, while torsion captures vertical deviations. Analyzing these parameters supports the understanding of turbulence, diffusion mechanisms, and energy transfer processes in the atmosphere or hydrosphere.

Finally, in data science and complex systems modeling, geometric representations based on the Frenet frame have emerged as a means of describing nonlinear trajectories in multidimensional spaces. For instance, in epidemic modeling, financial forecasting, or solar wind dynamics, curvature and torsion can characterize the “geometric behavior” of a time series curve, identifying regions of rapid change (high curvature) or structural transformation (high torsion). Thus, the Frenet frame provides a bridge between geometric abstraction and dynamic system interpretation.

Now, one can observe the results of the discussion. In the results, segmentation of the models is managed using 12-hour frames. A new segment is created every 12 hours to establish the curve model.

Table **5** displays the actual values, estimated values, and the average error of these values for some random segments for Germany. In this table, the parameter u indicates which parameter is used to obtain the predicted score. The word "index" here indicates the selected day of the relevant segment. For example, 2(5) means the 5th day of the 2nd segment.

As can be seen from Table **5**, regardless of which segment and index are randomly selected, the estimated score is obtained with minimum error.

For Germany: The results of the Bézier curve model for active case data from Germany are significant and satisfactory. The average error of this model is 0.112951%. The maximum error is also observed in the model at 1.5532%. The results obtained by a classical differential geometric approach without normalizing the case numbers are comparable to modern computer-aided applications. Fig. (**3**) shows active cases, Bézier model, and their average error. The average error specified by the formula Error $= 100.\left|\frac{\text{active case}-\text{estimated case}}{\text{active case}}\right|$.

Table 5: Particular segments, values with curve parameter, and average errors for Germany.

Segment (Index)	Actual Value	Estimated Value	u	Average Error (%)
1(4)	16	16.003	0.999	0.018731
2(5)	130	129.973	0.875	0.021042
3(11)	12327	12340.43	0.762	0.108931
4(3)	22364	22348.37	0.888	0.069876
5(1)	66885	66800.33	0.001	0.126591
6(2)	125452	125467.1	0.916	0.012012
6(8)	141397	141391.5	0.244	0.003858
7(6)	157770	257757.5	0.001	0.007949

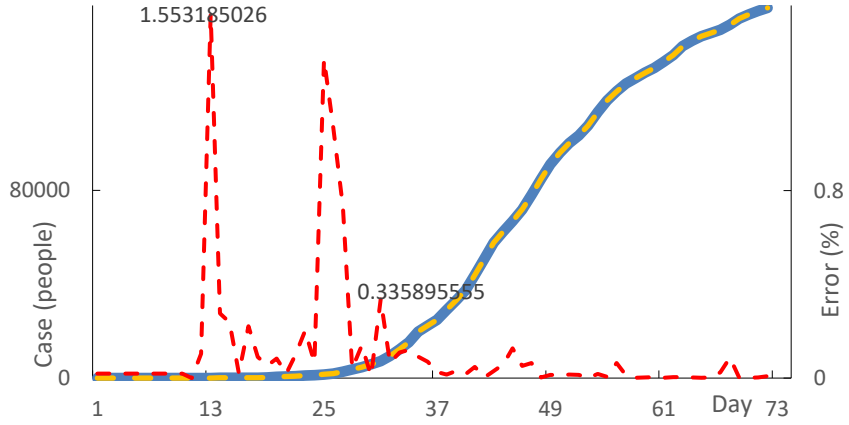

Figure 3: Germany model and its error.

Table **6** displays the actual values, estimated values, and the average error of these values for some random segments for Canada. In this table, the parameter u indicates which parameter is used to obtain the predicted score.

Table 6: Particular segments, values with curve parameter, and average errors for Canada.

Segment (Index)	Actual Value	Estimated Value	u	Average Error (%)
1(2)	8	8.003497	0.999	0.043706
2(3)	15	15.02	0.946	0.133339
3(5)	142	141.7095	0.893	0.204577
4(4)	1470	1469.308	0.916	0.047061
4(10)	5655	5651.359	0.178	0.064383
5(7)	15512	15510.5	0.426	0.009641
6(9)	33383	33388.74	0.243	0.017208
7(5)	46895	46882.76	0.145	0.000928

For Canada: The results of the curve model for active case data from Canada are substantial and suitable. The average error of this model is 0.08685%. The maximum error is also observed in the model at 1.1837%. The results found without normalizing the case numbers are comparable to modern computer-aided applications. Fig. (**4**) displays active cases, curve model, and their average error.

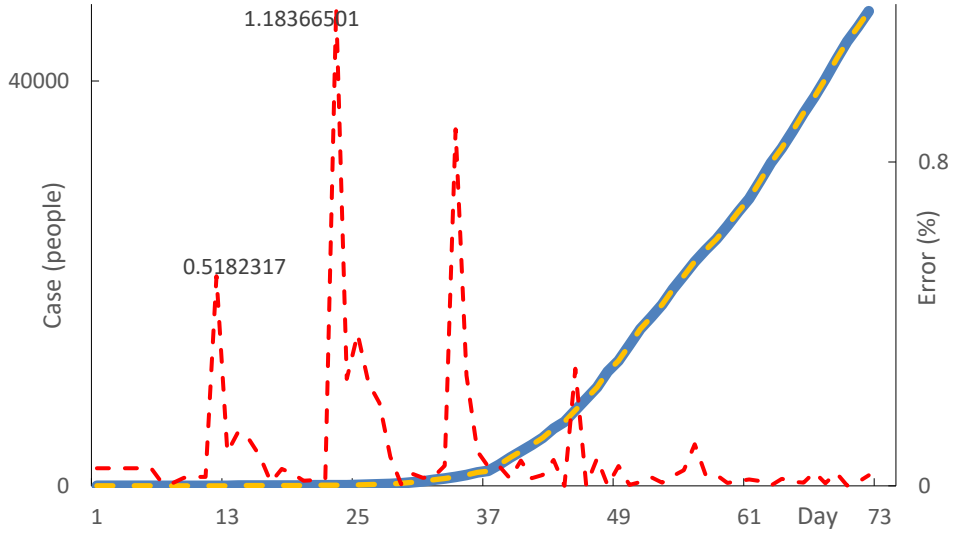

Figure 4: Canada model and its error.

Table **7** displays the actual values, estimated values, and the average error of these values for some random segments for Israel. In this table, the parameter u indicates which parameter is used to obtain the predicted score.

Table 7: Particular segments, values with curve parameter, and average errors for Israel.

Segment (Index)	Actual Value	Estimated Value	u	Average Error (%)
1(3)	1	1.000999	0.999	0.099999
2(2)	3	2.994196	0.972	0.193450
3(6)	143	143.1946	0.772	0.136073
4(9)	3035	3033.751	0.308	0.041153
5(4)	6857	6854.781	0.701	0.032354
5(11)	9968	9966.79	0.062	0.012138
6(7)	12758	12758.14	0.338	0.001073
7(4)	15058	15058.26	0.269	0.001711

For Israel: The results of the curve model for active case data from Israel are substantial and suitable. The average error of this model is 0.11283%. The maximum error is also observed in the model at 1.8232%. The results found without normalizing the case numbers are comparable to modern computer-aided applications. Fig. (**5**) displays active cases, curve model, and their average error.

For China: All results can be compared with China. This country's results of the curve model for active case data are important and acceptable. The average error of this model is 0.82209%. The maximum error is also observed in the model at 1.5532%. The results obtained by a classical differential geometric approach without normalizing the case numbers are comparable to modern computer-aided applications. Fig. (**6**) shows active cases, Bézier model, and their average error.

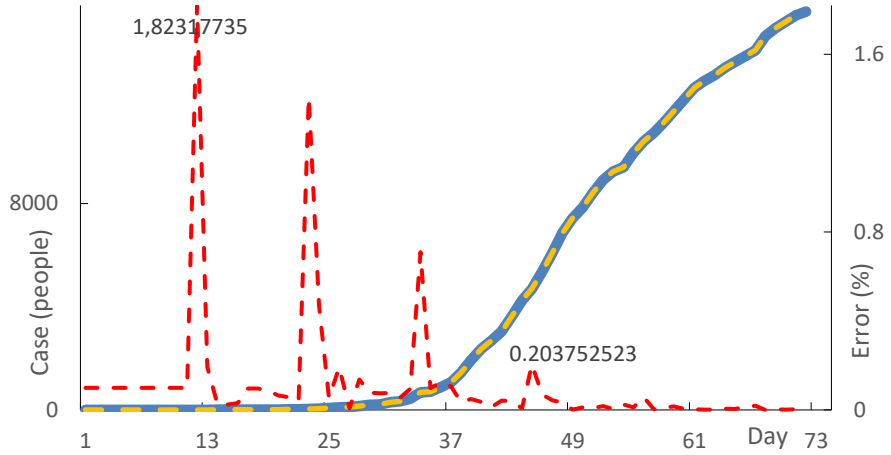

Figure 5: Israel model and its error.

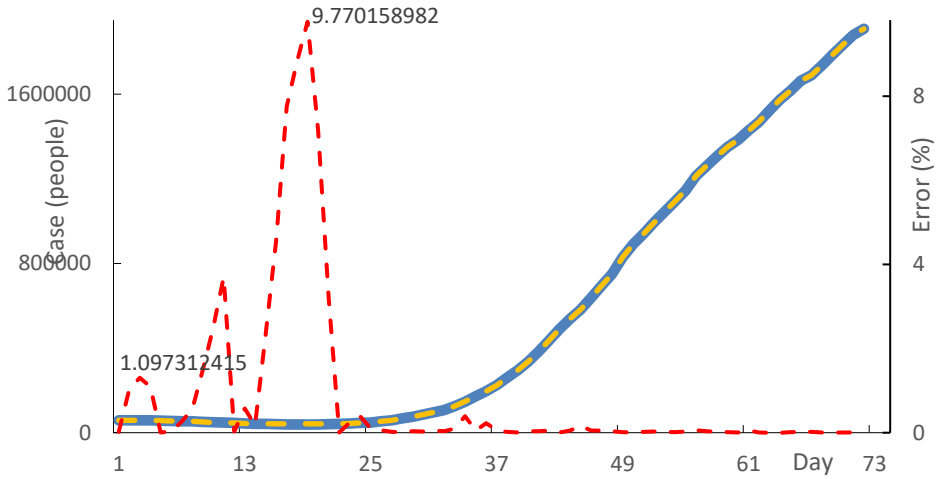

Figure 6: China model and its error.

One can immediately realize that the model for China's active cases has a slightly higher error compared to the other countries mentioned. At this point, the adaptable, adjustable segmented structure of the Bézier curve comes into play. In the data segment with the highest error, the segmentation is reduced from 12 hours to 6 hours, and the model is remodeled. First, the second 12 hours are divided into two 6-hour segments. Fig. (**7**) illustrates the average error for this discussion.

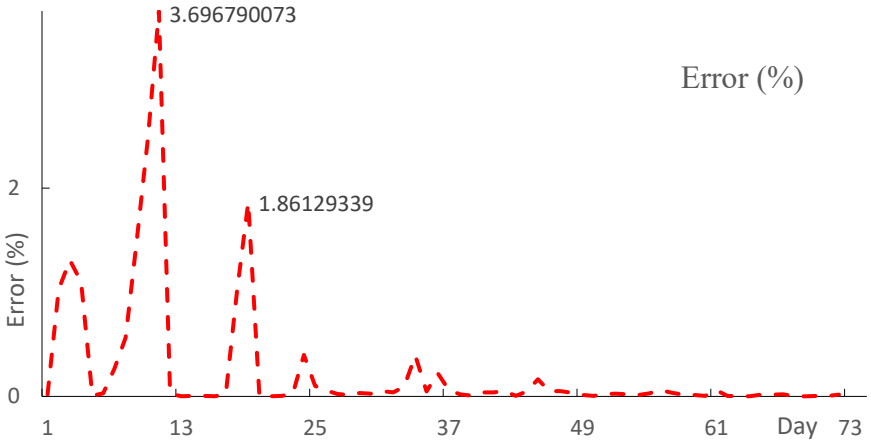

Figure 7: Average error for China model after six hours piece wise decomposition for second segment.

It should be noted that with this intervention, the average error immediately decreased from 0.82209% to 0.24237% and maximum error from 9.7702% to 3.6968%.

After this intervention, if the first 12 hours of data are divided into two segments (6 hours each), the result in Fig. (**8**) is displayed.

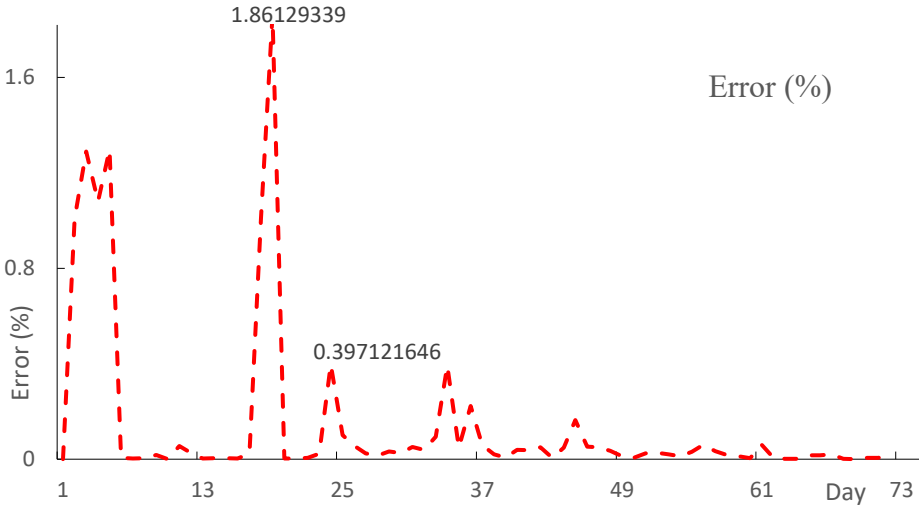

Figure 8: Average error for China model after six hours piece wise decomposition for first and second segment.

One can note that with this intervention, the average error immediately decreased from 0.242365% to 0.14178% and maximum error from 3.6968% to 1.8613%.

Table **8** displays the actual values, estimated values, and the average error of these values for some random segments for China. In this table, the parameter u indicates which parameter is used to obtain the predicted score. In this piecewise approach, one can see six hours segmentation for the estimation model.

Table 8: Particular segments, values with curve parameter, and average errors for China.

Segment (Index)	Actual Value	Estimated Value	u	Average Error (%)
1(1)	57990	57989.56	0.999	0.000755
2(2)	54418	54419.58	0.354	0.002896
3(3)	42262	42263.95	0.511	0.004624
3(4)	41297	41295.51	0.697	0.003597
4(4)	39433	39433.98	0.062	0.002490
4(5)	40947	40948.15	0.560	0.002813
5(5)	59168	59182.06	0.833	0.023764
6(6)	294801	294821.5	0.654	0.006960
7(7)	940105	939881.7	0.416	0.023749
8(11)	1663676	1663954	0.037	0.016704
9(2)	1735696	1735731	0.844	0.002032

Real-time estimation of epidemiological indicators is essential for early intervention, resource allocation, and public health decision-making during pandemics. The proposed Bézier curve framework is particularly suited for real-time monitoring because of its low computational cost, deterministic structure, and independence from complex parameter calibration. The segmented C^0-continuous formulation allows health authorities to update

estimates as new data become available, even in irregular reporting conditions. Since the model does not rely on stochastic assumptions, it can rapidly produce stable projections that support decisions such as adjusting containment measures, predicting hospital demand, or planning logistics before critical thresholds are reached.

3.1. Limitation and Future Works

Although the Bezier-based prototype demonstrates extremely low error rates, several limitations should be acknowledged. First, the model is sensitive to abrupt fluctuations or reporting inconsistencies, as geometric continuity may be affected by noise in input data. While segmentation can mitigate this issue, overly frequent segment breaks may reduce interpretability. Second, the current formulation is tailored to pandemics with relatively smooth temporal progression; diseases with multi-wave or highly erratic propagation patterns may require additional constraints or higher-order continuity conditions (e.g., C^1 or C^2). Third, the approach assumes that case reporting follows a monotonic temporal structure, which may not hold for all epidemiological systems. Future work may focus on integrating adaptive smoothing, noise-aware preprocessing, or curvature-based anomaly detection to improve robustness in heterogeneous data environments.

4. Conclusions

The COVID-19 pandemic has had profound and lasting effects on the world. It has long-term effects on health, the economy, and society. Countries are implementing various strategies to limit the effects of the pandemic. In this sense, each country's approach varies depending on its health infrastructure, resources, and social structure. On the other hand, the pandemic also provides important lessons on global cooperation, strengthening health systems, and preparing for future pandemics. This study introduces a Bézier curve–based geometric prototype capable of representing the temporal evolution of pandemic dynamics with remarkable precision. The model's parametric structure and piecewise continuous C^0 segmentation enable a flexible yet stable estimation of active COVID-19 cases. Its geometric continuity allows the curve to capture the intrinsic trajectory of epidemic propagation without dependence on stochastic or noise-prone datasets. Applications to Germany, Canada, and Israel demonstrated a mean absolute error as low as 0.087%, confirming the robustness and generalizability of the geometric formulation. The simplicity of the Bézier parametrization, coupled with its computational efficiency, provides a valuable foundation for constructing predictive manifolds and curvature-based analyses in future epidemiological modeling. Consequently, the presented framework offers a mathematically consistent, cost-free, and adaptable approach for real-time epidemic monitoring and strategic decision-making.

Conflict of Interest

The author declares no conflict of interest.

Funding

The study received no financial support.

Data Availability

All data is gathered from the worldometer (https://www.worldometers.info/).

Acknowledgment

None.

References

[1] Ciotti M, Ciccozzi M, Terrinoni A, Jiang WC, Wang CB, Bernardini S. The COVID-19 pandemic. Crit Rev Clin Lab Sci. 2020; 57(6): 365-88. https://doi.org/10.1080/10408363.2020.1783198

[2] Yang L, Liu S, Liu J, Zhang Z, Wan X, Huang B, *et al*. COVID-19: immunopathogenesis and immunotherapeutics. Signal Transduct Target Ther. 2020; 5: 128. https://doi.org/10.1038/s41392-020-00243-2

[3] Yuki K, Fujiogi M, Koutsogiannaki S. COVID-19 pathophysiology: a review. Clin Immunol. 2020; 215: 108427. https://doi.org/10.1016/j.clim.2020.108427

[4] Satici MO, Islam MM, Satici C, Uygun CN, Ademoglu E, Altunok I, *et al*. The role of a noninvasive index 'SpO_2/FiO_2' in predicting mortality among patients with COVID-19 pneumonia. Am J Emerg Med. 2022; 57: 54-9. https://doi.org/10.1016/j.ajem.2022.04.036

[5] Kumawat S, Bhatter S, Suthar DL, Purohit SD, Jangid K. Numerical modeling on age-based study of coronavirus transmission. Appl Math Sci Eng. 2022; 30(1): 609-34. https://doi.org/10.1080/27690911.2022.2116435

[6] Kisa S, Kisa A. A comprehensive analysis of COVID-19 misinformation, public health impacts, and communication strategies: scoping review. J Med Internet Res. 2024; 26: e56931. https://doi.org/10.2196/56931

[7] Agrawal H, Singh A, Sharma H, Purohi SD. Age-based investigation of COVID-19 prevalence in Ethiopia using mathematical modelling. South East Asian J Math Math Sci. 2024; 20(1): 297-312. https://doi.org/10.56827/SEAJMMS.2024.2001.23

[8] Akyol K. ETSVF-COVID19: efficient two-stage voting framework for COVID-19 detection. Neural Comput Appl. 2024; 36: 18277-95. https://doi.org/10.1007/s00521-024-10150-0

[9] Tan CY, Jang ST, Lam SM, An AQ, Lo UK. Teaching and learning challenges due to the COVID-19 pandemic: a systematic review. Educ Res Rev. 2025; 47: 100667. https://doi.org/10.1016/j.edurev.2025.100667

[10] Garg T, Rakshit M, Manivel M, Shyamsunder S. Modeling of hepatitis B virus transmission with vaccination, treatment, and memory effects. Adv Theory Simul. 2025; e01358, epub ahead. https://doi.org/10.1002/adts.202501358

[11] Soni K, Kumawat S, Sinha AK. Fractional-order model for Marburg virus transmission: assessing the impact of awareness, burial and cremation practices. Beni-Suef Univ J Basic Appl Sci. 2025; 14: 109. https://doi.org/10.1186/s43088-025-00691-1

[12] Eroglu E, Esenpinar AA, Bozkurt E, Tek S. Mathematical modeling of COVID-19 phenomenon; the cases: Germany, Israel, and Canada. Fresen Environ Bull. 2020; 29(10): 9063-74.

[13] Baysazan E, Berker AN, Mandal H, Kaygusuz H. COVID-19 modeling based on real geographic and population data. Turk J Med Sci. 2023; 53(1): 333-9. https://doi.org/10.55730/1300-0144.5589

[14] Bansal R, Mittal P, Verma P. Impact of social media during COVID-19 using binary logistic model. In: Market Dynamics and Strategies in a Post-Crisis World: Navigating a World in Flux. 2025. p.129-38. https://doi.org/10.1142/9789811292101_0011

[15] Shyamsunder S, Bhatter K, Jangid A, Abidemi K, Owolabi KM, Purohit SD, *et al*. A new fractional mathematical model to study the impact of vaccination on COVID-19 outbreaks. Decision Anal J. 2023; 6: 100156. https://doi.org/10.1016/j.dajour.2022.100156

[16] Shen Y, Liu F, Zhang W. Real-time forecasting of COVID-19 spread according to protective behavior and vaccination: an ARIMA model approach. BMC Public Health. 2023; 23: 16419. https://doi.org/10.1186/s12889-023-16419-8

[17] Santos F, Alonso J. Modeling pandemic behavior with a network-SIRD approach. Cent Eur J Oper Res. 2023; 31: 1085-102. https://doi.org/10.1007/s10100-023-00894-w

[18] Ramírez A, Ochoa M. COVID-19 pandemic trend modeling and analysis to support resilience decision-making. Biology. 2023; 9: 156. https://doi.org/10.3390/biology9070156

[19] Martínez L, Vega P. Analysis and simulation of epidemic COVID-19 curves with the Verhulst model applied to statistical inhomogeneous age groups. Mathematics. 2024; 12: 5858. https://doi.org/10.3390/math12045858

[20] Patzina A, Collischon M, Hoffmann R, Obrizan M. Mental health in Germany before, during and after the COVID-19 pandemic. PLoS One. 2025; 20: e0313689. https://doi.org/10.1371/journal.pone.0313689

[21] Michaelsen S, Jordan SP, Zarowsky C, Koski A. Challenges to the provision of services for sexual and intimate partner violence in Canada during the COVID-19 pandemic: results of a nationwide web-based survey. Violence Against Women. 2025; 31: 1536-56. https://doi.org/10.1177/10778012241228286

[22] Haimi M, Shadmi E, Hornik-Lurie T, Sperling D. Telehealth usage disparities in Israel in light of the COVID-19 pandemic: retrospective cohort study of intersectional sociodemographic patterns and health equity implications. J Med Internet Res. 2025; 27: e77600. https://doi.org/10.2196/77600

[23] Guan Y, Guang L, Li L, Liu Y. The rally effect of the COVID-19 pandemic and the White Paper Movement in China. J Contemp China. 2025; 34: 117-28. https://doi.org/10.1080/10670564.2024.2356863

[24] Fuchs A, Kaplan L, Kis-Katos K, Leue S, Turbanisch F, Wang F, *et al*. Mask wars: sourcing a critical medical product from China in times of COVID-19. J Int Econ. 2025; 155: 104068. https://doi.org/10.1016/j.jinteco.2025.104068

[25] Wang W, Luo X, Ren Z, Fu X, Chen Y, Wang W, *et al*. Impact of COVID-19 pandemic measures on hospitalizations and epidemiological patterns of twelve respiratory pathogens in children with acute respiratory infections in southern China. BMC Infect Dis. 2025; 25: 103. https://doi.org/10.1186/s12879-025-10463-y

[26] Bézier PE. Numerical control-mathematics and applications. Translated by Forrest AR, Pankhurst AF. John Wiley; 1972.

[27] Rogers DF, Adams JA. Mathematical elements for computer graphics. 2nd ed. New York: McGraw-Hill; 1990.

[28] Ozturk G. k-sabit eğriler (Master's thesis). Karadeniz Technical University, Institute of Science; 2019. Turkish.

[29] Erkan E. Öklid düzleminde ve Öklid uzayında Bézier eğrileri (PhD thesis). Yildiz Technical University, Institute of Science; 2019. Turkish.

[30] Eroglu E. Bézier cubics' agreement with the neural network of the TEC map. Soft Comput. 2024; 28: 10835-52. https://doi.org/10.1007/s00500-024-09863-0

[31] Eroglu E, Tretyakov OA. The Bézier curve and neural network model of the time-domain transient signals. Comput Phys Commun. 2024; 301: 109211. https://doi.org/10.1016/j.cpc.2024.109211

[32] Kılıçoğlu Ş, Şenyurt S. On the cubic Bézier curves in E3. Ordu Univ J Sci Technol. 2019; 9(2): 83-97.